Integrated Antenna for Second Generation Emergency Radio Beacons of the COSPAS-SARSAT System

S.N. Boyko, *Cand. Sci. (Physics and Mathematics), bosnik2012@yandex.ru*
A branch of "ORKK"-"NII KP", Moscow, Russian Federation
A.V. Isaev
A branch of "ORKK"-"NII KP", Moscow, Russian Federation
D.S. Kosorukov
A branch of "ORKK"-"NII KP", Moscow, Russian Federation
Yu.S. Yaskin, Cand. Sci. (Engineering)
A branch of "ORKK"-"NII KP", Moscow, Russian Federation

Abstract. A built-in antenna for distress beacons of the second generation for search and rescue COSPAS-SARSAT system that consists of a Huygens element in the form of a combined half-wave frame (loop) and dipole is proposed. The formation of the radiation pattern in the cardioid form is achieved by specific excitation of the dipole and loop. An engineering design methodology of the antennas is developed and the comparison of the results of numerical simulation with experimental data is presented. The performance of the antenna meets the requirements of COSPAS-SARSAT to the second generation beacons on a frequency of 406 MHz. An example of application of the developed antenna in the personal distress beacon with its placing on the inner side of the side wall of the frame with the dimensions of 200×75×45 mm is given. The main advantages of this antenna are easy manufacture, protection from external mechanical effects, and low cost.

Keywords: dipole-loop antennas, cardioid pattern, hemispherical radiation pattern, built-in antennas

Introduction

The international search and rescue system COSPAS-SARSAT was established in 1977 for the purpose of distress alerting and the location of personal radio beacons and radio beacons installed on watercraft and aircraft in the event of an emergency. Up to now, the system was based on a low-orbit satellite constellation, and the main type of antenna for transmitting a signal to a satellite at a frequency of 406 MHz was a monopole. The main direction of the development of the COSPAS-SARSAT system is currently the creation of a space segment based on the MEOSAR medium-orbit satellites to create uniform coverage of the entire visible hemisphere of the sky in any part of the globe, which will allow continuous spatial and temporal monitoring of the activated beacon search zone. As a consequence, the main requirement for the antennas of second-generation beacons is the formation of a hemispherical (cardioid) radiation pattern (RP) with linear or circular polarization, the maximum of which is directed to the zenith.

The design of antennas with a cardioid RP shape for personal radio beacons proves to be quite a challenge, since the beacons themselves must have small dimensions and mass. The Expert Group of the COSPAS-SARSAT Committee considered the known types of antennas (spiral, microstrip, planar F-antennas and L-antennas) with a hemispherical shape of the radiation pattern and came to a disappointing conclusion about the inapplicability of these antennas in the personal radio beacons of the second generation: either the dimensions and mass exceed the permissible limits, or the efficiency of radiation is insufficient. Thus, there was no variant of the antenna applicable in the second-generation personal radio beacons.

The search for a solution to this difficult problem by the employees of the NII KP research institute led to a constructive version of the integrated antenna for second-generation beacons, which has acceptable dimensions, mass and DN in the form of a cardioid. This result is achieved due to the combination of a dipole and a shortened loop antenna, which is a practical implementation of the Huygens element.

The algorithm of calculating the dipole-loop antenna with the cardioid shape of the radiation pattern is presented in the article, the stages of its design are described in detail, and the results of computer simulation are compared with the measured characteristics of the antenna model at a frequency of 406 MHz.

Algorithm for calculating an embedded antenna for second generation beacons

The idea of forming a spherical radiation pattern in the form of a Huygens element was described in many monographs, such as [1]. The Huygens element is an elementary source of unidirectional radiation formed by orthogonal in-phase electric and magnetic dipoles. The field of the Huygens element in the far zone is a spherical wave, and the RP does not depend on the angle φ, and in any plane $\varphi = const$ is determined by the expression $F(\theta) = 1 + \cos\theta$.

The basic implementation of such an antenna, which has a loop antenna with a perimeter equal to the wavelength λ in free space, is not applicable in second-generation beacons because of the large dimensions.

The paper [2] sets forth the theoretical basis for the formation of a cardioid-type radiation pattern with a dipole-loop pair provided that the dimensions of all the radiators are much smaller than the wavelength. In [3], a design variant of an antenna for mobile communication with a RP in the form of a cardioid is proposed, which is a combination of an asymmetric dipole and an electrically small loop, energized in quadrature relatively to the dipole (each arm). However, in [3] the material is illuminated briefly, as a consequence the method for calculating a dipole-loop antenna with a half-wave frame is not presented. The authors of this article tried to fill this gap.

The design of this antenna was taken by us as a basis, in which the changes necessary for this particular application were made.

A schematic diagram of the antenna design is shown in Fig. 1, a. A truncated loop with a perimeter of $\lambda/2$ contains three containers, one of which is included in the center of the loop, and two others - at the beginning of its two arms. The inclusion of capacitance C_1 in the antinode of the voltage makes it possible to shorten the loop with a perimeter equal to the wavelength λ to a loop with a perimeter equal to half the wavelength [4], however, the input impedance of such a frame at the operating frequency will be inductive. To compensate for the inductive component of the input impedance, the capacitances C_2 and C_3 included at the input of the frame. The frame emitter in this form is practically a half-wave dipole with a capacitive load, wound into a loop, fed by a current.
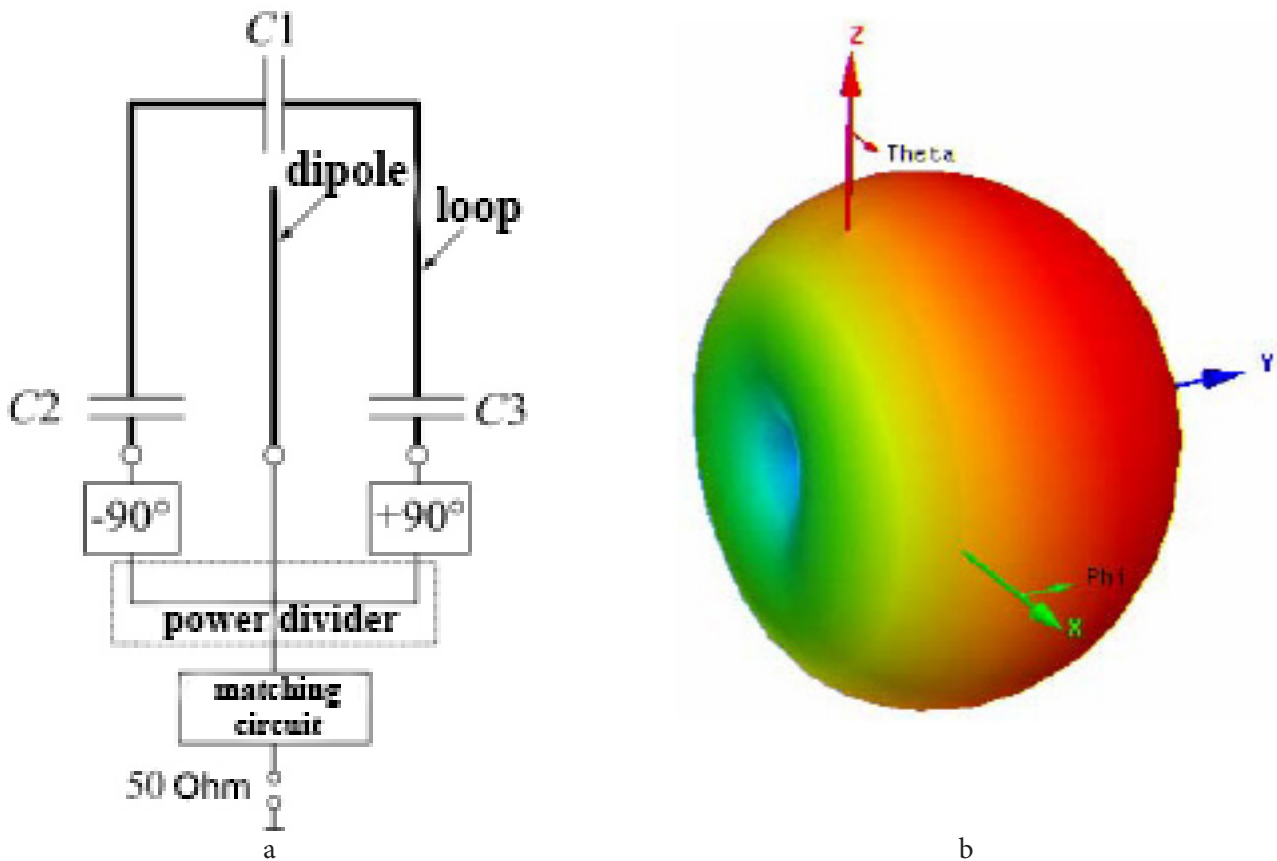
Fig.1. Schematic diagram of the antenna (a) and the shape of the dipole-loop antenna radiation pattern (b)

In [3] it was noted that for the formation of a spherical radiation pattern of an antenna, the dimensions of all radiators of which are much smaller than the wavelength, it is necessary to observe the following conditions:

1) the centers of emission of the dipole and the loop must coincide, while the mutual influence between the emitters should be minimized;

2) the powers emitted by the dipole and the loop must be equal to each other;

3) the currents flowing in the dipole and the loop must have a phase difference of 90°.

If these conditions are met, the antenna will have a directional diagram in the form of a cardioid with a maximum radiation in the direction of the branch of the frame, energized with a phase of + 90° relative to the dipole, and a minimum radiation in the reverse direction (Fig. 1b).

Antenna consists of several elements, and its calculation and design is a complex task, which must be divided into several stages. We used the following algorithm for designing such an antenna:

Step 1. The calculation of an asymmetric dipole on a printed circuit board is carried out separately;

Step 2. The calculation of a half-wave loop on a printed circuit board is carried out separately;

Step 3. A microstrip power divider is designed with loads in the output arms equal to the calculated resistance of the dipole and loop radiation, provided that the powers of the signals entering the loop and the dipole are equal;

Step 4. Calculation of the balancing transformer on lumped elements is carried out;

Step 5. Calculation of the antenna assembly;

Step 6. The line-building-out network of the antenna is calculated.

Step 7. Optimization of the relative positioning of the antenna and the radio beacon transceiver board is carried out in order to minimize the effect of the board on the form of the RP.
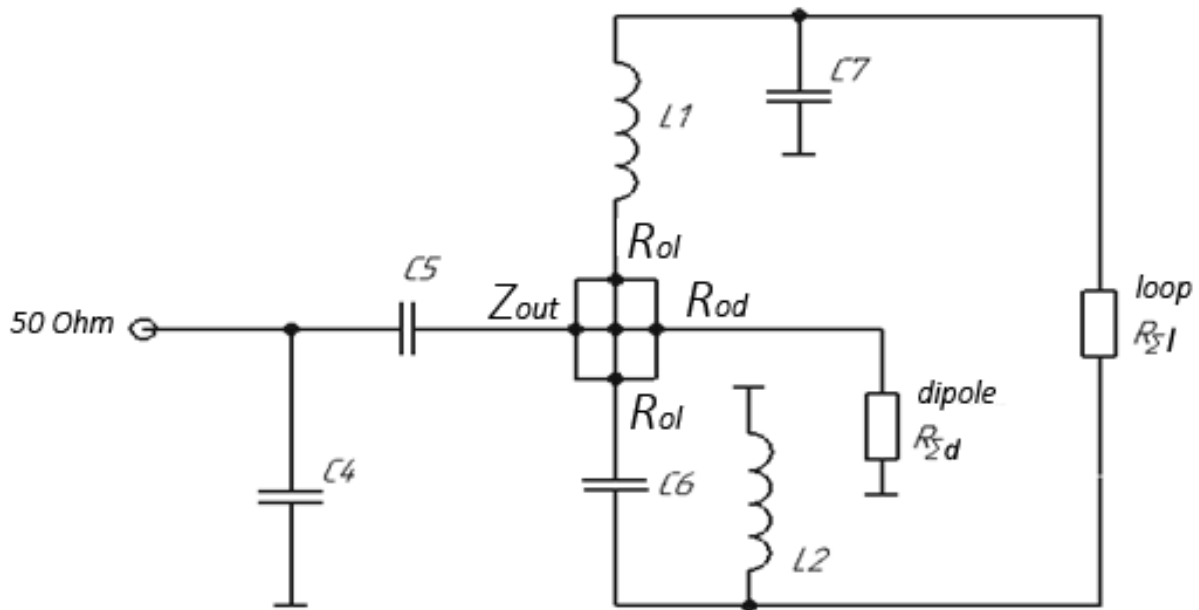
Fig.2. The electric circuit of the dipole-loop antenna

The electrical circuit of the combined antenna is shown in Fig. 2. The diagram shows that the dipole is connected directly to the power divider, and the loop arms are energized with a phase shift of ±90° relative to the dipole through a balanced-unbalanced transformer formed by the pairs of lumped elements L_1, C_7 and C_6, L_2. In this case, the shoulders of the loop are energized opposite in phase to each other. The capacitive L-section matches the input impedance of the antenna with a 50-ohm path.

At the first stage of antenna design, it is necessary to calculate the dimensions of an asymmetrical dipole consisting of a quarter-wave emitter and a coaxial ground plane (counterweight), which are located on one side of the printed circuit board (Fig. 3). In this case, the emitter is located strictly along the longitudinal axis of the board. On the same side of the board is a power divider.

At the next stage, a loop for a working frequency of 406 MHz is designed. The loop antenna is made in the form of a strip on the back side of the printed circuit board along its external contour so that the dipole radiator is located inside the frame on its axis (Fig. 3), which is due to the first condition for the formation of the cardioid type RP above. The perimeter of the frame is a constructive parameter that is determined mainly by the

length of the dipole radiator and the width of the board, dictated also by the first condition for the formation of cardioid type RP.

Values of capacitances C_1, C_2, C_3 are calculated by the long-line method applied to the equivalent circuitry of the loop antenna at the resonant frequency (Fig. 4, a).

The loop antenna is replaced by a long line of two conductive strips of width w spaced a distance a, which is loaded at the end by the capacitance C_1 and the radiation resistance $R_{\Sigma}l$. The power fed to the loop input is calculated using the resistance transformation formula along the transmission line [5]:

$$z(b) = z_{\mathrm{w}} \frac{\dot{z}_{_н} + j z_{\mathrm{w}} \, tg \, \beta l}{z_{\mathrm{w}} + j \dot{z}_{_н} tg \, \beta l},$$
(1)

where Z_{w} is the wave impedance of the transmission line, $\dot{z}_i = R_{\Sigma p} - \dfrac{j}{\omega C_1}$ is the load impedance, l is the length of the transmission line, $\beta = \dfrac{2\pi}{\lambda}$ is the wavelength constant of empty space.

The radiation resistance of the loop $R_{\Sigma p}$ is found by the formula [6]:

$$R_{\Sigma p} = 197 \cdot (\Pi_p / \lambda)^4,$$
(2)
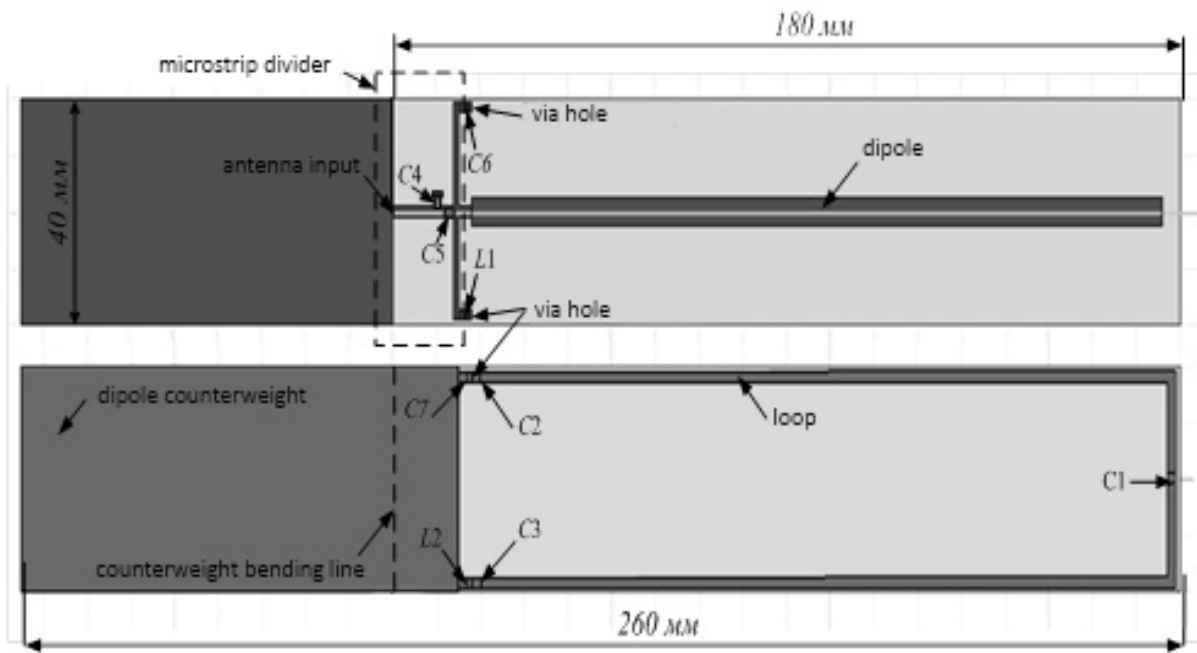
Fig.3. Antenna topology: top and bottom sides of the board
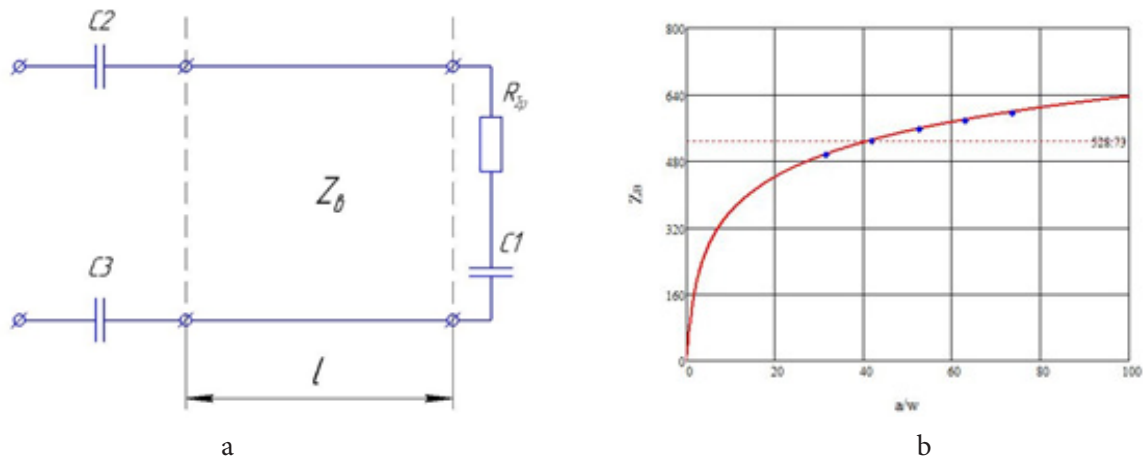
Fig.4. Equivalent circuit of the loop antenna (a); dependence Zw on a/w (b)

where P_l is the perimeter of the loop.

The wave impedance of the transmission line can be determined from the expression for Z_w a two-wire transmission line [5]:

$$z_B = 276\lg\left(a/d + \sqrt{1+(a/d)^2}\right),\qquad(3)$$

where d is the diameter of the wire, assuming that the width of the conductive strip w is equal to twice the value of d, i.e.

$$w = 2d\qquad(4)$$

Relation (4) is determined empirically, namely by comparing the values Z_w calculated from formula (3) with the values obtained with strict electrodynamic calculations. The dependence of the wave resistance of a two-wire transmission line Z_w on the magnitude of a/w is shown in Fig. 4, b the solid line is the graph $z_B(a/w)$ calculated by formulas (3), (4), the points are the calculations of z_B in the software package HFSS15 for the width of the strip w = 1.9 mm and a number of values of the distance between the strips a = {28 ; 38; 48;

58; 68} mm; It can be seen that the calculation according to formula (3) assuming (4) completely agrees with the values of the wave impedance obtained with strict electrodynamic calculations.

After recalculation $\dot{z}_i$ to the input of the loop by the formula (1), the nominal values of the elements C_1, C_2, C_3 are found from the condition that the imaginary parts of the total resistance of the loop are equal to zero:

$$\text{Im}\{\dot{z}(b)\} + \frac{1}{j\omega C_2} + \frac{1}{j\omega C_3} = 0 \qquad (5)$$

When the elements C are equal, the equation has two unknown parameters: $C_2 = C_3 = C$ and C_1. This indicates that the nominal value of one of the elements can be specified, and the second one is found from the solution of equation (5). Figure 5 shows a plot of C as a function of C_1, which was obtained by numerically solving equation (5). This graph can be used to select a pair of matching capacitors $\{C_1, C\}$.
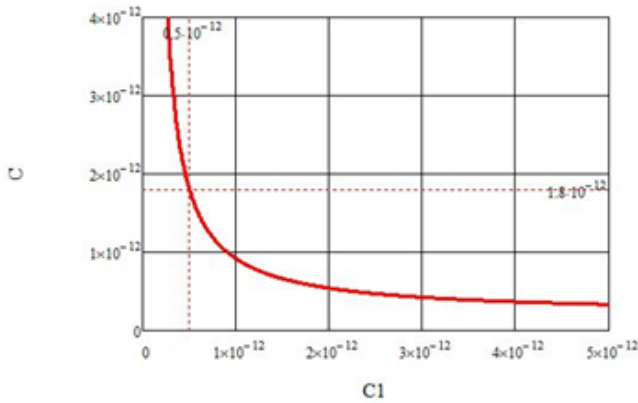
Fig.5. The calculated dependence of C on C1

Calculation of the power divider is carried out from the condition of equality of powers radiated by the loop and the dipole (the second condition for the formation of a cardioid type RP):

$$P_{\sum p} = P_{\sum Д}$$

$$\text{or } I_{a\_p}{}^2 \cdot R_{\sum p} = I_{a\_Д}{}^2 \cdot R_{\sum Д} \qquad (6)$$

where $I_{a\_Д}$ and I_{a_p} are the effective values of the dipole current and the loop at the connection points.

The resistance of the radiation of the loop $R_{\sum p}$ is given by the previously given formula (2), and the resistance of the dipole radiation is [1]:

$$R_{\sum Д} = 80\pi^2 \cdot (l_Д / \lambda)^2, \qquad (7)$$

where $l_Д$ is the length of the dipole.

Taking into account (2), (7) and (6), we obtain a formula for the ratio of the currents at the points of connection of the dipole and loop antennas:

$$\frac{I_{a\_Д}}{I_{a\_p}} = \sqrt{\frac{R_{\sum p}}{R_{\sum Д}}}. \qquad (8)$$

When designing a power divider, the relation for power is used. Since the input power is proportional to the square of the current, the expression for the ratio of input powers is:

$$m = \frac{P_{âx\_Д}}{Đ_{âx\_ð}} = \left(\frac{I_{a\_Д}}{I_{a\_p}}\right)^2 = \frac{R_{\sum p}}{R_{\sum Д}}. \qquad (9)$$

The alignment of the loop arms with ports 2 and 3 of the divider is performed using a balanced-unbalanced transformer, its arms are essentially a high-pass filter (HPF) and a low-pass filter (LPF), which in addition to the phase-shifting circuit function also play the role of resistance transformers [5].

The characteristic impedance Z_p of a length of a long line equivalent to the stages of the LPF and HPF, ensuring the transformation of the loading resistance R to the input resistance R_{0l} is [7]:

$$Z_П = \sqrt{2R_{0p}\frac{R}{2}} = \sqrt{R_{0p}R} = \sqrt{\frac{L}{C}} \qquad (10)$$

In addition, the following condition must be met:

$$f_0 = \frac{1}{2\pi\sqrt{LC}}, \qquad (11)$$

where f_0 is the center frequency of the operating range.

From the formulas (12) and (13) we obtain formulas for calculating the L and C elements that make up the balanced-unbalanced transformer:

$$L_1 = L_2 = \frac{Z_П}{2\pi f_0}, \qquad (12)$$

$$C_6 = C_7 = \frac{1}{2\pi f_0 Z_П}. \qquad (13)$$

If the L and C elements are equal in the arms of the balanced-unbalanced transformer, the HPF specifies a phase shift of minus 90 degrees, and the LPF shifts the

| a | b |
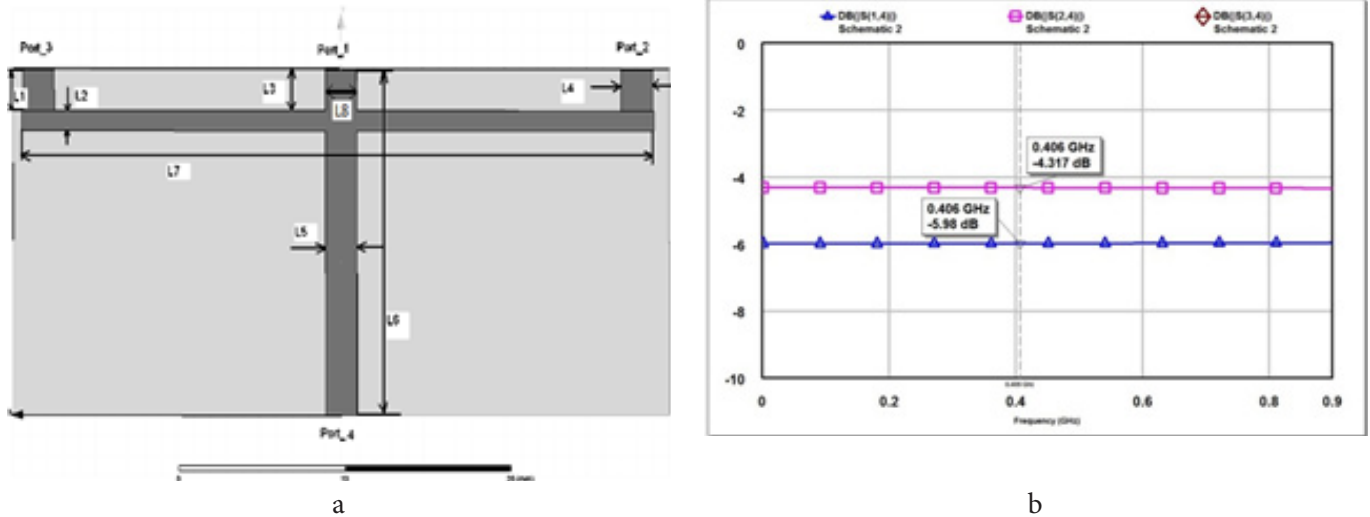
Fig.6. Topology of the microstrip power divider (a); the dependence of the moduli of the transmission coefficients on the frequency (b)

phase by plus 90 degrees. Thus, the third condition for the formation of a hemispherical (cardioid) radiation pattern is met automatically.

Calculation of the dipole-loop antenna

As the material of the antenna board was chosen FR-4 glass fiber 1 mm thick with a relative permittivity $\varepsilon_r = 4.4$. According to the calculation performed with the software package HFSS15, the length of an asymmetric vibrator with a resonant frequency of 406 MHz for a strip width of 5 mm was 162 mm with a counterweight of 100x40 $(mm)^2$. Taking into account the length of the asymmetric dipole, the calculated perimeter of the loop was P_l = 366 mm with a loop width a = 38 mm and a loop length l = 164 mm. As a result, the overall dimensions of the antenna board, taking into account the counterweight, were 260 mm (length) x 40 mm (width).

For the selected width, the loop strip w = 1.9 mm at a = 38 mm, the calculated value of the loop wave impedance calculated from formulas (3), (4) was z_B = 528.73 Ohm.

For the dimensions of the asymmetrical dipole and the loop given above, formulas (2), (7) and (9) calculate the values of the radiation resistance and the power division coefficient: $R_{\sum \dot{A}} = 37.5$ Ohm, $R_{\sum p} = 12$ Ohm, m = 0.32. As a result, the power divider must divide the input power in the following ratios:

$$P_{\text{вх}\_Д} = 0.25 \cdot P_{\text{вх}}$$

$$P_{\text{вх}\_p1} = P_{\text{вх}\_p2} = 0.375 \cdot P_{\text{вх}},$$

where $P_{\text{вх}\_p1}, P_{\text{вх}\_p2}$ is the power coming into each shoulder of the loop.

The power division is executed using microstrip lines. The topology of the power divider is shown in Fig. 6, a. The loop is connected to the power divider through segments of identical microstrip lines, and the dipole is connected directly to the breakout of the power divider. Loads of the three outputs of the divider are the radiation resistances of the loop $R_{\sum p}$ (half of each output of the divider connected to a loop arm) and the dipole $R_{\sum \dot{A}}$.

The criteria for the synthesis of the power divider were conditions (10), (11), namely, the modulus of the transmission coefficient between the divider input (port 4) and the dipole connection point (port 1) is equal to $|s_{14}| = -6$ dB; The transmission coefficient modules between the divider input and the connection points of the loop arms (ports 2 and 3) are equal to $|s_{24}| = |s_{34}| = -4.3$ dB. The required power splitting was achieved by selecting the width $L2$ and the length $L7$ of two identical microstrip lines in the arms of the power divider. As a result of the synthesis, the following widths and lengths of the intermediate transmission lines were obtained: $L2$ = 0.01 mm, $L7$ = 38 mm.

Due to the technical impossibility to manufacture divider arms 0.01 mm in width, it was decided to increase the $L2$ value to a physically realizable value of 0.5 mm. With this topology, the output impedance of port 1 is

a   b
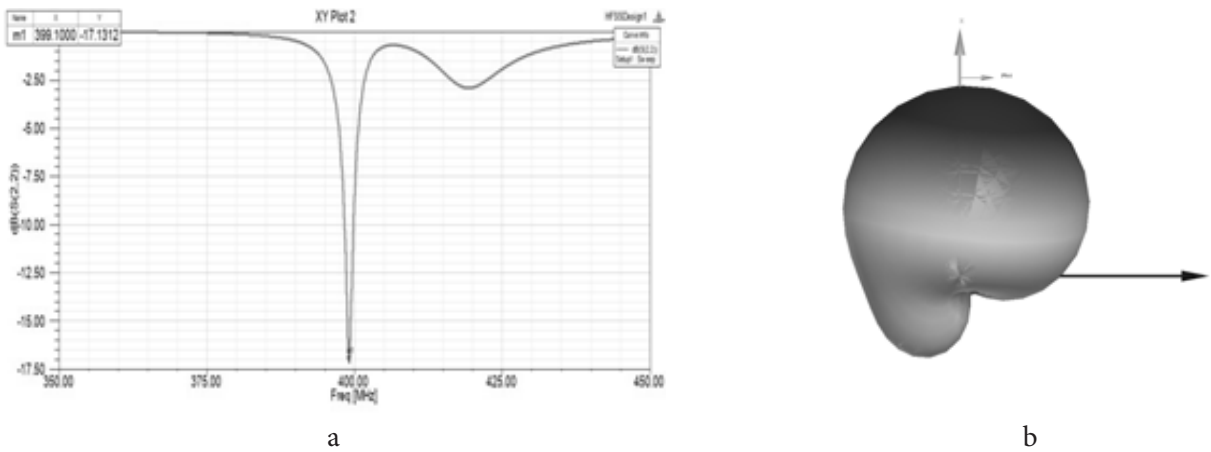
Fig.7. Calculated characteristics of the antenna: a - the modulus of the reflection coefficient at the antenna input;
b - radiation pattern at resonant frequency

a   b
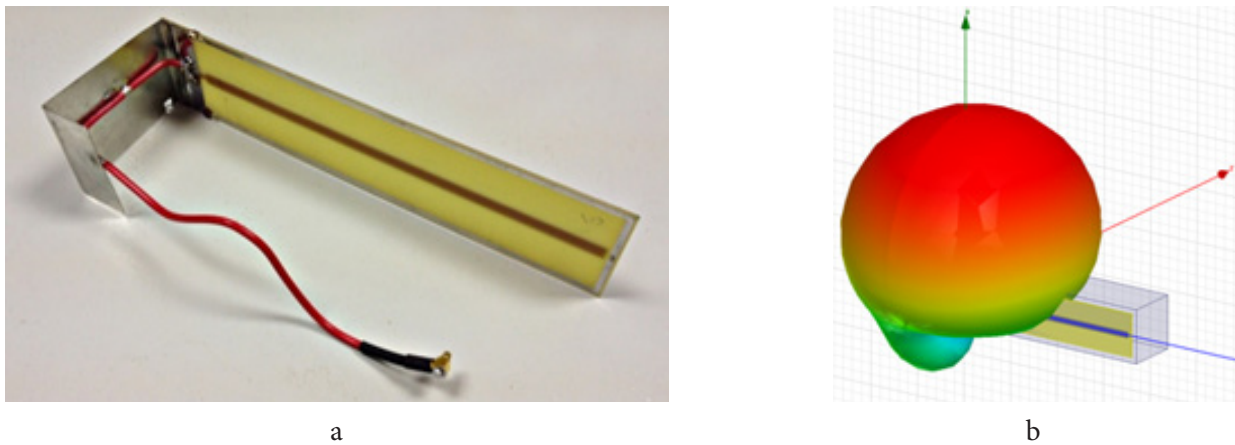
Fig.8. Dipole-frame antenna model (a); form of RP during operational position of the antenna (b)

R_{0d} = 200 Ohm, and the output impedances of ports 2 and 3 are R_{0l} = 72.5 ohms each. For these values of load resistances, the necessary power division is provided (the calculated dependences of the transmission coefficient moduli on frequency are shown in Fig. 6 *b*), but it becomes necessary to match the radiation resistance of the dipole and the loop with the above-mentioned resistances of outputs (ports) of the power divider.

The matching of the dipole with port 1 of the divider was achieved by introducing a step transition with a width L8 = 2 mm and a length L3 = 4 mm.

The matching of the loop with ports 2 and 3 of the power divider is carried out using a matching-balancing transformer. The nominal values of the lumped elements of the loop transformer are calculated by the formulas (10) - (13) for the load resistance $R=R_{\Sigma l}/2 = 6$ Ohm, calculated by formula (1) of the input resistance of the loop, R_{0l}=72.5 Ohm, were: $L_1=L_2$= 4.7nH, $C_6=C_7$=32.6 pF.

Calculation of the input impedance of the antenna assembly (dipole + loop with a balanced-unbalanced transformer + power divider) was carried out in the software package HFSS15. The calculated value of the input impedance was $z_{âõ} = 8 + j6$ Ohm. Since the input impedance has a low value of the active component and a non-zero value of the inductive component, a matching transformer is needed to match the antenna input to the 50-ohm path. In our case, it was implemented in the form of a L-shaped matching circuit, consisting of a serial and parallel capacitances. The calculation of these capacitances was carried out according to the method described in [8], [9]. As a result, the capacitance values were: C_4=15 pF, C_5= 7.5 pF.

The calculated reflection coefficient $|s_{11}|$ at the antenna input and its radiation pattern are shown in Fig. 7 (*a*) and 7 (*b*), respectively. The modulus of the reflection coefficient at the resonant frequency is -26 dB, which
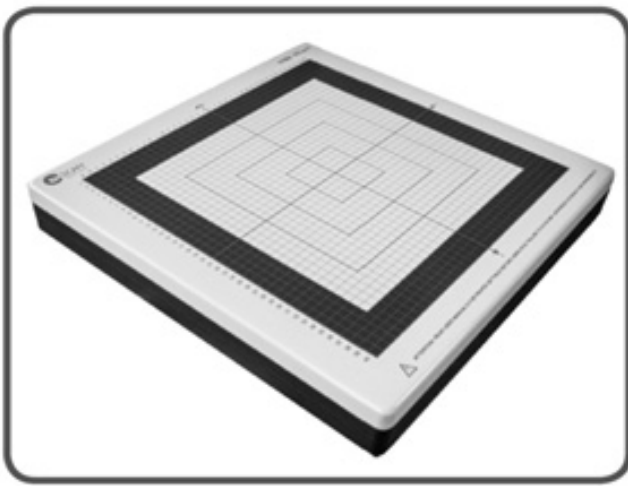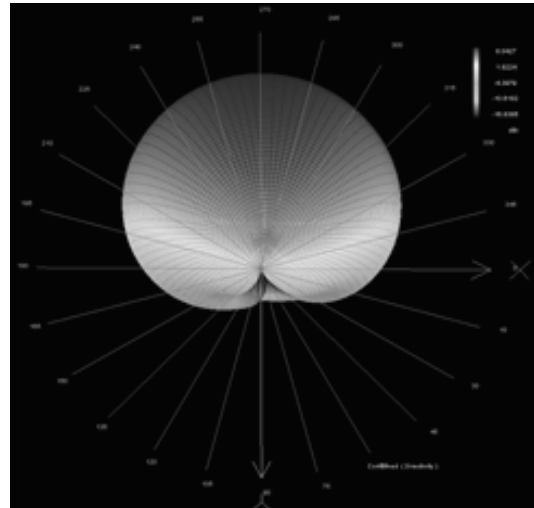
a   b

Fig.9. Photo of the RFxpertRFX2 scanner (a) and the type of PR of the dipole-frame antenna measured
on the scanner (b)
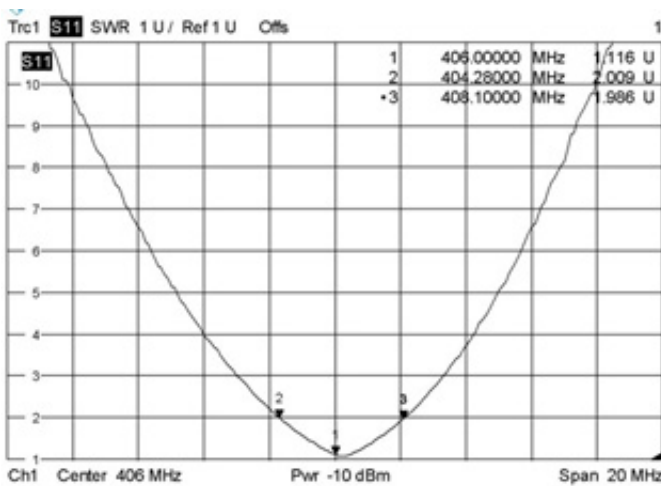
Fig. 10. The experimental frequency dependence of the
VSWR at the antenna input

corresponds to the input VSWR = 1.1. The K_u value of the antenna at the maximum of the RP was 2.8 dB. It can be seen from Fig. 7 (b) that in the lower part of the diagram there is a small parasitic radiation, which is connected with the presence of a counterweight to the antenna, which is undesirable for the frame emitter.

On this the antenna design process could be considered complete, but the resulting longitudinal antenna size (260 mm) is clearly large and does not allow it to fit into the dimensions of the personal radio beacon. Therefore, in order to incorporate the antenna into the

beacon casing, the counterweight of the dipole was bent at an angle of 90 degrees to the board in such a way that the longitudinal dimension of the board with the topology of the antenna does not exceed 180 mm (the fold line is shown in Fig. 3). In the simulation, it was determined that with such a counterweight configuration, the changes in the shape of the radiation pattern are negligible and can be compensated for by a small change in the capacitances C_6, C_7 in the frame matching circuits.

The results of measurements of the prototype of the antenna and comparison with the calculated data

To test the proposed technique for designing a dipole-loop antenna, a model was made, consisting of an antenna board and a counterweight connected to it. The antenna board was made on a material of FR-4 (ε_r= 4,4) with a thickness of 1 mm, the counterweight was made of tinned sheet 0.2 mm thick. The topology of the antenna board is made according to the calculations carried out by the algorithm described above. The matching capacitors C_1, C_2, C_3 were selected according to the chart in Fig. 5 and are equal to: $C_2 = C_3 = 1.8$ pF, $C_1 = 0.5$ pF (dotted markers in Figure 5). Other options are also possible C_1, C_2, C_3 according to the chart in Fig. 5, for example: $C_1 = 0.25$ pF, $C_2 = C_3 = 3$ pF or $C_1= 1$ pF, $C_2 = C_3 = 0.9$ pF.- The capacitors in the balanced-unbalanced transformer are variable to fine-tune the phase difference in the loop

a   b
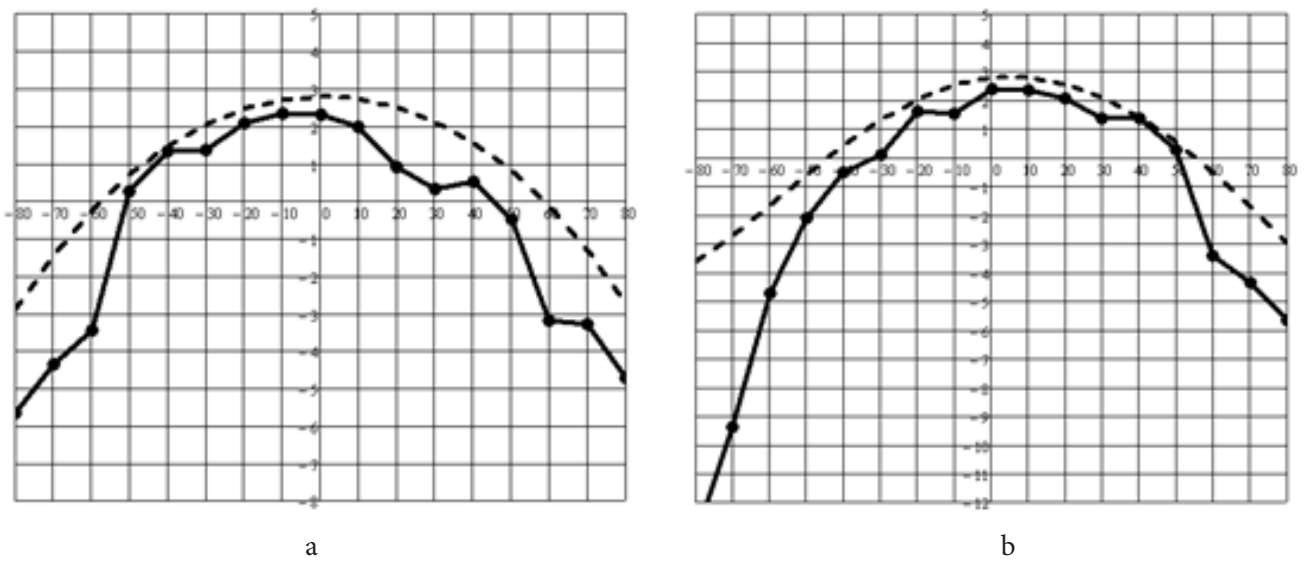
Fig.11. Measured in the anechoic chamber (solid lines) and calculated (dotted lines) antenna RP: a - for φ = 0 °,
b - for φ = 90 °
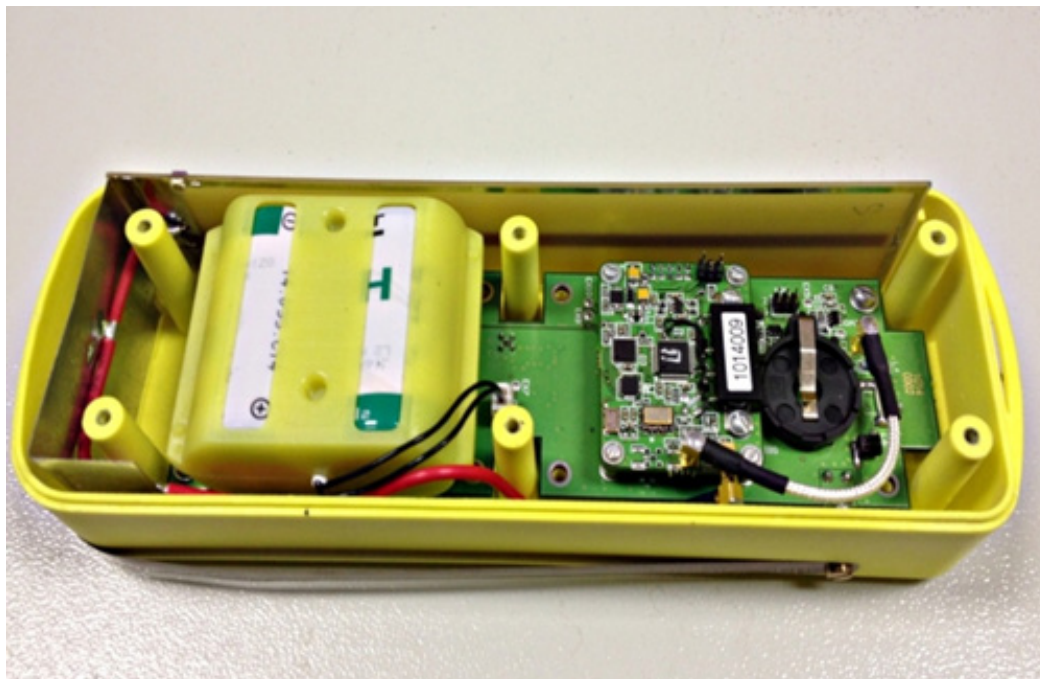
Fig.12. Dipole-frame antenna in the beacon housing

arms. The photograph of the antenna layout is shown in Fig. 8 (a), the calculated three-dimensional RP in the operational position of the antenna is shown in Fig. 8 (b). An additional (second) bending of the antenna's counterweight at an angle of 90 degrees is due to the need to incorporate the antenna into the projected body of the second generation personal radio beacon. The antennas are located on three narrow sides of a rectangle with dimensions (180x65x40) mm³.

The final testing and tuning of the antenna was carried out by the form of RP with the RFxpertRFX2 scanner by EMScan, which allows to determine the shape of the antenna radiation pattern in real time directly at the workplace [10]. This device measures the near field of the antenna and recalculates it into a far zone field with a RP display in three-dimensional form with a sufficient accuracy for tuning the antenna. The combined antenna was placed on the working surface of the scanner by

the plane of the board (counterweight up), then a small adjustment of the capacitances C_6, C_7 was made in the balanced-unbalanced transformer to achieve a cardioid shape of the RP. A photograph of the scanner and the radiation pattern of the antenna measured with it are shown in Fig. 9, *a* and 9, *b*, respectively. Then, the VSWR and PR of the scanner-tuned antenna were measured in the far zone in an anechoic chamber.

The measured dependence of the VSWR at the antenna input on the frequency is shown in Fig. 10.

It follows from the figure that at the operating frequency of 406 MHz the value of the VSWR is 1.1, which fully coincides with the calculated value. The RP of the antenna in the upper hemisphere at φ=0° and 90°, measured in an anechoic chamber, are shown in Fig. 11 (a) and 11 (b), respectively. Also in these figures, the dashed line shows the results of calculating the RP in the software package HFSS15. The measured value of gain at the maximum of the RP is 2.5 dB, and the calculated value is 2.8 dB. From the above analysis it can be seen that a good rate of coincidence of the calculated and experimental data has been achieved.

It should be noted that according to the requirements of the COSPAS-SARSAT standard on the second-generation radio beacons in 90% of the radiation pattern, the antenna gain should be in the range from minus 7 to plus 4 dB for elevation angles from 15 ° to 90 °. The obtained experimental values of gain (θ) satisfy this requirement: the values of gain vary in the range from minus 6 dB to plus 2.5 dB in a given range of angles (see Figure 11).

When the antenna is placed inside the radio beacon its board is located along one of its long side walls, and the counterweight is along the adjacent short side wall, with a small overlapping with the opposite long wall (Fig. 12).

Since there is a transmitter-receiver board perpendicular to the antenna board in the radio beacon, it was necessary to measure its effect on the characteristics of the antenna. Therefore, computer simulation and experiments determined the best position of the transmitter-receiver board with respect to the antenna board for the operation of the antenna, in which the shape of the RP is retained (Fig. 8, b*).

The dipole-loop antenna has several advantages as a built-in antenna. Firstly, because of the lack of radiation in the lower hemisphere, it makes it possible to reduce the negative influence of the underlying surface on the DN shape. Secondly, it is protected from external mechanical influences by the radio beacon housing. Thirdly, it has a simple manufacturing technology and low cost.

Conclusion

In this article:

• A dipole-frame antenna is proposed for use in the new (second) generation of the COSPAS-SARSAT personal rescue beacon.

• A detailed description of the design stages of such an antenna is given and an engineering procedure for its calculation is proposed.

• The input standing wave ratio of the antenna (SWR = 1.1) and the hemispherical RP of the antenna at a frequency of 406 MHz with a gain = 2.5 dB were calculated experimentally.

• By changing the configuration of the counterweight, the antenna is embedded in the radio beacon with dimensions $(200 \times 75 \times 45)$ mm³.

• The influence factor of the transmitter board on the form of the antenna RP is taken into account. Its best position in the radio beacon casing is chosen.

References

1. *Fradin A.Z. Antenno-fidernye ustroystva* [Antenna feeder devices]. Moscow, "Svyaz'", 1977. (in Russian)

2. Vendik O.G., Pakhomov I.A. Electric- and magnetic-field strengths in the Fresnel zone of a microradiator formed by an electric and a magnetic dipole. *Technical Physics*, 2005, Vol. 50, No. 11, pp. 1479–1484.

3. Turalchuk P.A., Kholodnyak D.V., Vendik O.G. Novel low-profile antenna with hemispherical coverage suitable for wireless and mobile communications. *2008 Loughborough Antennas & Propagation Conference.* 17-18 March 2008, Loughborough, UK, pp. 337–340.

4. Turkin N. Elektricheski ukorochennaya ramochnaya antenna [Electrically shortened frame antenna]. *Radio* [Radio]. 2002, No. 12, pp. 58–59. (in Russian)

5. Sazonov D.M. *Antenny i ustroystva SVCh* [Microwave antennas and devices]. Moscow, Vyssh. shk., 1988, 432 p. (in Russian)

6. Rotkhammel' K. Entsiklopediya antenn. [Encyclopedia about antennas]. Moscow, DMK Press, 2011, 814 p. (in Russian)

7. Zheksenov M.A., Petrov A.S. Skhemy na LC-elementakh, prednaznachennye dlya vozbuzhdeniya turniketnykh izluchateley, sostoyashchikh iz trekh elektricheskikh i trekh magnitnykh dipoley [LC circuits designed for excitation of turnstile radiators consisting of three electric and three magnetic dipoles]. *Radiotekhnika i elektronika* [Journal of Communications Technology and Electronics]. 2014, Vol. 59, No. 4, pp. 289–293. (in Russian)

8. Petrov A.S., Kovaleva M.V. Soglasovanie vkhodnogo impedansa korotkogo monopolya s volnovym soprotivleniem trakta pri pomoshchi G-zvena, sostoyashchego iz induktivnostey s konechnoy dobrotnost'yu [Matching of the input impedance of the monopole with the wave impedance of the path by means of a Γ-link made of inductances with finite Q factor]. *Radiotekhnika i elektronika* [Journal of Communications Technology and Electronics]. 2012, Vol. 57, No. 4, pp. 418–421. (in Russian)

9. Available at: http://www.emscan.com/